



Since January 2020 Elsevier has created a COVID-19 resource centre with free information in English and Mandarin on the novel coronavirus COVID-19. The COVID-19 resource centre is hosted on Elsevier Connect, the company's public news and information website.

Elsevier hereby grants permission to make all its COVID-19-related research that is available on the COVID-19 resource centre - including this research content - immediately available in PubMed Central and other publicly funded repositories, such as the WHO COVID database with rights for unrestricted research re-use and analyses in any form or by any means with acknowledgement of the original source. These permissions are granted for free by Elsevier for as long as the COVID-19 resource centre remains active.



NEOPLASTIC DISEASE

Feline Respiratory Extramedullary Plasmacytoma with Lymph Node Metastasis and Intrahistiocytic Amyloid

S. E. Sykes^{*}, V. Byfield[†], L. Sullivan^{*}, S. J. Bender^{*}, P. F. Moore[‡]
and M. D. Sánchez^{*}

^{*} Department of Pathobiology, University of Pennsylvania School of Veterinary Medicine, 3800 Spruce St, Philadelphia, Pennsylvania, [†] Red Bank Veterinary Hospital, 210 Route 206 S., Hillsborough, New Jersey and [‡] Department of Pathology, Microbiology and Immunology, School of Veterinary Medicine, University of California (Davis), Davis, California, USA

Summary

A 14-year-old domestic longhaired cat presented with a 2-year history of nasal discharge and a recent onset of inappetence and submandibular lymphadenopathy. The cat was humanely destroyed after developing severe respiratory distress. Necropsy examination revealed thickened nasal turbinates and soft palate, and friable red–tan material within the frontal sinus, nasal cavity and nasopharynx. The lungs contained multifocal irregular friable tan nodules. Multiple lymph nodes were enlarged, friable and red–tan in colour. Histopathology revealed a mature type extramedullary plasmacytoma (EMP) within the frontal sinus, nasal cavity, soft palate, larynx, trachea, lungs and multiple lymph nodes. The lymph nodes and larynx also contained marked granulomatous inflammation with extensive intrahistiocytic (and lesser amounts of extracellular) lambda light chain amyloid, confirmed by electron microscopy and immunohistochemistry. Neoplastic cells expressed CD79a and MUM1. This is the first report of an infiltrative EMP of the feline respiratory tract with lymph node metastasis and predominantly intrahistiocytic amyloid.

© 2016 Elsevier Ltd. All rights reserved.

Keywords: amyloid; cat; extramedullary plasmacytoma; respiratory tract

Extramedullary plasmacytomas (EMPs) are monoclonal proliferations of terminally differentiated B cells that do not involve the bone marrow. An uncommon neoplasm in cats, the majority of cases are cutaneous (Majzoub *et al.*, 2003), although there are rare reports of non-cutaneous EMPs, including those of sinonasal (Schöniger *et al.*, 2007), gastrointestinal (Rowland and Linke, 1994; Zikes *et al.*, 1998), cerebral (Greenberg *et al.*, 2004), intraocular (Michau *et al.*, 2003), lip and gingival origin (Kyriazidou *et al.*, 1989). With the exception of the intracerebral and sinonasal cases, most EMPs are described as well-circumscribed, non-infiltrative masses (Majzoub *et al.*, 2003; Greenberg *et al.*, 2004;

Schöniger *et al.*, 2007). Additionally, although primary local extracellular amyloidosis with secondary granulomatous inflammation is well-reported in plasma cell dyscrasias in animals (Rowland and Linke, 1994; Majzoub *et al.*, 2003; Gross *et al.*, 2005), extensive accumulation of intrahistiocytic amyloid is unusual.

A 14-year-old neutered male domestic longhaired cat was presented to a referral hospital for a 2-year history of haemorrhagic nasal discharge and a recent onset of submandibular swelling and inappetence. Physical examination revealed marked submandibular lymphadenopathy, but additional diagnostic tests were initially declined by the owner. The cat showed no response to empirical treatment with prednisolone and clindamycin. Cytology of an aspirate taken from the submandibular lymph nodes 1 month after initial

Correspondence to: S. E. Sykes (e-mail: sykessa@vet.upenn.edu).

presentation revealed predominantly macrophages, admixed with lymphocytes, plasma cells and a few neutrophils and eosinophils. The macrophages were distended with magenta-coloured material that was amorphous and curvilinear to granular. The cytology was interpreted as inflammatory, with reactive lymphoid hyperplasia and increased numbers of plasma cells.

A complete blood cell count revealed a mild neutrophilia ($10.3 \times 10^9/l$, reference interval $2.5\text{--}8.5 \times 10^9/l$) and monocytosis ($0.64 \times 10^9/l$, reference interval $0.0\text{--}0.6 \times 10^9/l$). A serum biochemistry panel, measurement of total thyroxine concentration and chest radiographs were unremarkable. The urine protein:creatinine ratio was elevated (1.3, normal ≤ 0.5). Urine was not available for electrophoresis. The cat was negative for feline leukemia virus (FeLV) antigen, feline immunodeficiency virus (FIV) antibody, feline coronavirus (immunofluorescence [IFA]), *Toxoplasma* spp. IgM and IgG, *Cryptococcus* spp. antigen and *Neospora* spp. (IFA). Computed tomography (CT) of the head revealed mild nasal turbinate loss with severe thickening of the nasal mucosa, enlarged submandibular, medial retropharyngeal, superficial and deep cervical lymph nodes, and fluid and/or soft tissue in the frontal sinus and left tympanic bulla. Thoracic CT revealed several irregular soft tissue nodules throughout the pulmonary parenchyma and enlarged tracheobronchial lymph nodes.

Incisional biopsy samples of the frontal sinus and nasal turbinates revealed extensive plasmacytic infiltrates admixed with lymphocytes. Surgical excisional biopsy of the left submandibular lymph node revealed dense plasmacytic and histiocytic infiltrates with abundant intrahistiocytic, and lesser amounts of extracellular, congophilic material. Gram and acid-fast stains were negative and the intrahistiocytic material was weakly positive on periodic acid–Schiff staining. The lymph node findings were suggestive of a metastatic plasmacytoma, while the frontal sinus and nasal cavity findings were difficult to interpret (reactive versus neoplastic). The cat was represented 2 months after the initial presentation due to progressive respiratory distress, at which time it was humanely destroyed.

On necropsy examination, the nasal turbinates and soft palate were diffusely thickened and tan in colour. Soft, friable tan–pale red material filled approximately 80% of the frontal sinus, nasopharynx and the caudal half of the nasal cavity, obscuring the caudal nasal turbinates bilaterally (Supplementary Fig. 1). The left tympanic bulla contained viscous, slightly opaque pale yellow fluid. The tonsils were bilaterally mottled red–tan and the aryepiglottic folds and cuneiform processes of the larynx were bilaterally

enlarged, slightly nodular and mottled red–tan. The submandibular, medial retropharyngeal and superficial cervical lymph nodes were enlarged bilaterally, as well as the tracheobronchial and cranial mediastinal lymph nodes. On cut section, all of these lymph nodes were markedly friable and mottled red–tan, with complete loss of corticomedullary distinction. The lungs were slightly oedematous with multifocal, irregular, 0.2–1 cm diameter, friable, tan-coloured nodules throughout the parenchyma.

Histopathological examination revealed a round cell proliferation within the frontal sinus, left tympanic bulla, nasal turbinates, soft palate, larynx, trachea, lungs (predominantly surrounding bronchi), tonsil and the submandibular, retropharyngeal, superficial cervical, tracheobronchial, cranial mediastinal, pancreaticoduodenal and right colic lymph nodes. Neoplastic cells had a moderate amount of amphophilic cytoplasm, typically with a perinuclear halo and a round, eccentric nucleus with either hyperchromatic or finely stippled chromatin and 1–3 variably distinct nucleoli. The cells displayed mild to moderate anisocytosis and anisokaryosis, with occasional binucleation, and low numbers of mitoses (0–3 per $\times 400$ field) that were occasionally bizarre. These features were consistent with a mature type plasmacytoma (Fig. 1) (Majzoub *et al.*, 2003; Platz *et al.*, 1999). The neoplastic cells effaced the majority of the affected lymph nodes, with few lymphoid follicles remaining, and occasionally exhibited capsular invasion (not shown).

Admixed with the neoplastic cells within the lymph nodes and larynx was marked granulomatous inflammation, characterized by epithelioid macrophages and multinucleated giant cells, with extensive intrahistiocytic (and lesser amounts of extracellular) amorphous eosinophilic material (amyloid). Low numbers of lymphocytes, Mott cells and eosinophils were also scattered throughout affected lymph nodes. The amorphous eosinophilic intrahistiocytic (and extracellular) material was congophilic (Fig. 2), and exhibited apple-green birefringence under polarized light (not shown).

Additional findings in affected organs included mild to severe multifocal neutrophilic and histiocytic bronchitis with bronchiectasis and adjacent interstitial pneumonia, mild to severe secondary frontal bone and nasal turbinate osteolysis with fibrosis, haemorrhage and fibrinosuppurative erosive sinusitis/rhinitis, moderate secondary fibrinosuppurative erosive laryngotracheitis and otitis media. No evidence of neoplasia was identified within the bone marrow (left humerus and femur) or other internal viscera.

Immunohistochemistry (IHC) was performed using an Envision+ System™ (Dako, Carpinteria,

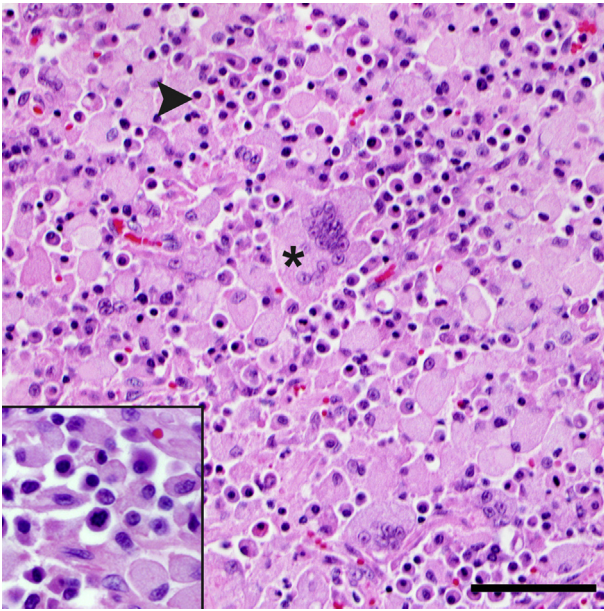


Fig. 1. Metastatic extramedullary plasmacytoma with intrahistiocytic amyloid within the retropharyngeal lymph node. Mature type neoplastic plasma cells (arrowhead) are admixed with many histiocytes and multinucleated giant cells with abundant intracellular amyloid (asterisk). HE. Bar, 25 μ m. Inset: higher magnification of the neoplastic plasma cells.

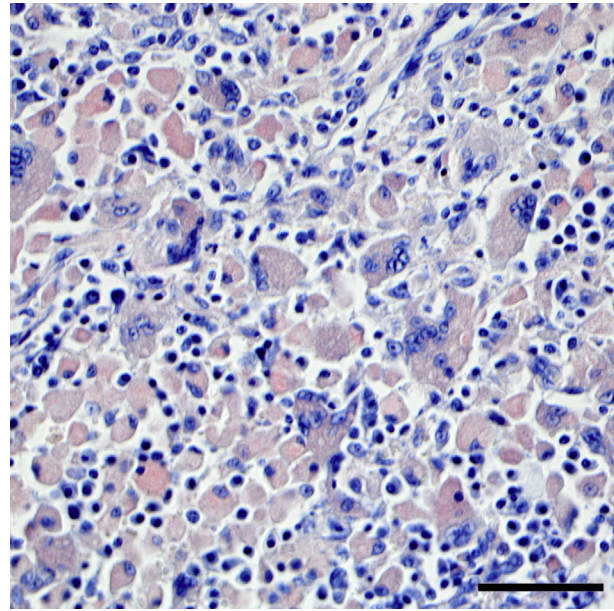


Fig. 2. Metastatic extramedullary plasmacytoma with intrahistiocytic amyloid within the retropharyngeal lymph node. Intrahistiocytic material is congophilic. Congo red. HE. Bar, 25 μ m.

California, USA). After dewaxing and pretreatment, target antigen retrieval was performed using a citrate buffer (pH 9.0 for CD79a and MUM1, pH 6.0 for SAA and both light chains). Sections were incubated with the following primary antibodies: mouse monoclonal antibodies against CD79a (1 in 500 dilution) and MUM1 (1 in 50 dilution) (each for 30 min), rabbit polyclonal antibodies against kappa (1 in 4,000 dilution) and lambda (1 in 12,000 dilution) light chains (each for 30 min) and canine AA (1 in 9,000 dilution; for 45 min) (Johnson *et al.*, 1995). Secondary detection was performed using a Dako Envision + / HRP™ kit, and secondary antibodies were mouse anti-mouse (for CD79a and MUM1) or goat anti-rabbit (for SAA and both light chains) (all from Dako). Antibody binding was 'visualized' using 3,3'-diaminobenzidine (DAB) as chromogen for CD79a and MUM1 and 3-amino-9-ethylcarbazole (AEC) as chromogen for SAA and the light chains. Positive controls included dog tonsils (for the light chains), a known positive renal amyloid case (for SAA) and a normal feline lymph node (for CD79a and MUM1). The negative controls consisted of a mouse (CD79a and MUM1) or rabbit (SAA and light chains) IgG isotype substitution for the primary antibodies used on the case tissues.

Neoplastic cells were CD79a⁺ and MUM1⁺ by IHC, and polymerase chain reaction for antigen re-

ceptor rearrangement (PARR) revealed a monoclonal rearrangement of the kappa deleting element (KDE) to a kappa variable segment (KDEv). IHC of the amyloid was moderately positive for lambda light chain (Fig. 3) and negative for serum amyloid A (SAA, not shown). The amyloid was occasionally slightly positive for kappa light chain, which was attributed to non-specific labelling that was not observed in the negative control, as the PARR results indicated that the neoplasm was lambda light chain restricted (the kappa locus was deleted, supporting the positive lambda IHC results).

Electron microscopy of the left submandibular lymph node revealed variably-sized intrahistiocytic membrane-bound aggregates of randomly-oriented non-branching 7.5–10 nm diameter fibrils with indeterminate length, which frequently displaced or indented the nucleus and other cell structures (Fig. 4). These findings were consistent with abundant intrahistiocytic amyloid (beta-pleated sheets of fibrils).

This case represents an extramedullary mature type plasmacytoma involving the upper and lower respiratory tract with lymph node metastasis. The patient was a geriatric male, consistent with the higher reported incidence of EMPs in older male cats (Majzoub *et al.*, 2003; Michau *et al.*, 2003; Greenberg *et al.*, 2004). Although the majority of human EMPs reportedly arise within the upper respiratory tract (dos Anjos Corvo *et al.*, 2013), this is a rare location in small animals, with only a few

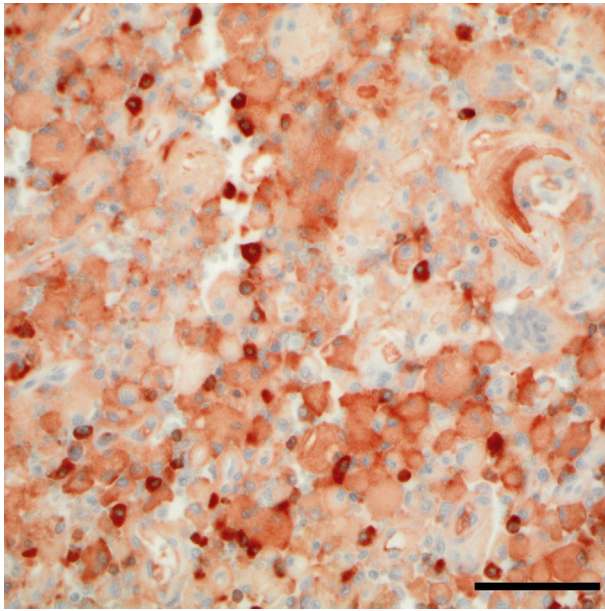


Fig. 3. Infiltrative extramedullary plasmacytoma with intrahistiocytic amyloid within the laryngeal mucosa. Intrahistiocytic material is moderately positive for lambda light chain. IHC. Bar, 25 μ m.

case reports describing primary laryngeal and tracheal EMPs in dogs, and one report involving the nasal cavity and frontal sinus of a cat (Chaffin *et al.*, 1998; Weigt and McCracken, 2001; Hayes *et al.*, 2007; Schöniger *et al.*, 2007; Witham *et al.*, 2012). This case is unique as it describes an EMP with extensive tissue infiltration as well as metastasis. In the previously reported case of sinonasal EMP in a cat, the neoplasm was limited to the nasal cavity and frontal sinus (Schöniger *et al.*, 2007). In the case of an intracerebral EMP in a cat, the neoplasm was more infiltrative, involving the leptomeninges, ventricular system, subependymal tissue and the habenular nucleus (Greenberg *et al.*, 2004). However, to our knowledge, the present case is the first report of extensive infiltration by an EMP within the upper and lower respiratory tract. Severe plasmacytic inflammation may be difficult to differentiate from a mature type plasmacytoma and initial biopsy and cytology samples from this cat were suggestive of an inflammatory process rather than neoplasia. Assimilation of necropsy findings with additional diagnostic tests allowed a diagnosis of a mature type EMP.

Amyloidosis may be categorized as primary (AL) or secondary (AA) depending on the pathogenesis. In domestic animals, primary amyloidosis typically develops in cases of plasma cell dyscrasias, although not all plasma cell dyscrasias result in amyloidosis. Neoplastic plasma cell populations may produce large quantities of monoclonal, complete or fragmented immunoglobulin light or heavy chains (typi-

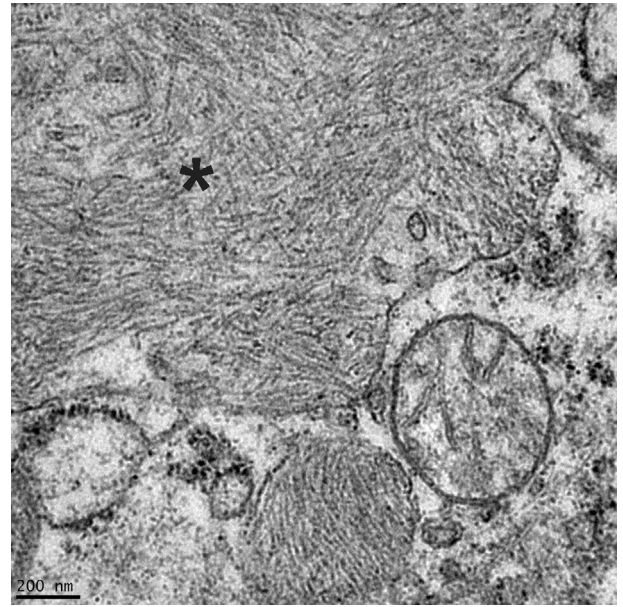


Fig. 4. Intrahistiocytic amyloid within the left submandibular lymph node. Abundant membrane-bound, randomly-oriented, non-branching, 7.5–10 nm diameter fibrils (asterisk) displace other organelles. Transmission electron microscopy.

cally lambda light chain in animals). In some cases, these proteins are unstable and insoluble and form aggregates of amyloid fibrils that are unable to be degraded by macrophages. Secondary amyloidosis is more common in animals and occurs in some cases of chronic inflammatory disease. The increased levels of inflammatory cytokines (specifically interleukin [IL]-1, IL-6 and tumour necrosis factor [TNF]- α) released by activated macrophages results in increased production and release of serum amyloid-associated peptide (SAA, an acute phase protein) by hepatocytes. SAA is degraded into a smaller AA protein, which is unstable, insoluble and prone to forming fibrils (amyloid). A defect in macrophage enzymes or a mutation in the SAA protein is theorized to result in amyloid accumulation, rather than the normal degradation of this acute phase protein (Snyder, 2012).

The deposition of amyloid (AL or AA) is often associated with secondary granulomatous inflammation (Rowland and Linke, 1994; Majzoub *et al.*, 2003; Gross *et al.*, 2005). There are occasional reports of intrahistiocytic amyloid in animal and human patients with primary amyloidosis, including rectal EMPs in dogs (Ramos-Vara *et al.*, 1998), a spinal plasmacytoma in a woman (Arnesen and Manivel, 1993) and a nasal EMP in a woman with cervical lymph node metastasis (Sharma *et al.*, 2009). However, the amyloid deposits in these reports was described as predominantly extracellular (or not specified),

making this the first report to describe predominantly intrahistiocytic amyloid (Arnesen and Manivel, 1993; Rowland and Linke, 1994; Ramos-Vara *et al.*, 1998; Majzoub *et al.*, 2003; Sharma *et al.*, 2009). We speculate that the preponderance of intrahistiocytic amyloid in this case may be due to the chronicity of the disease.

Acknowledgments

We thank T. D. O'Brien, University of Minnesota School of Veterinary Medicine, for performing the IHC; M. P. Sirivelu, Amgen Inc., South San Francisco, for assistance with the clinical pathology aspects of the case; and A. C. Durham, University of Pennsylvania School of Veterinary Medicine, for assistance with the images. Dr. Byfield's present affiliation is Mount Laurel Animal Hospital, Mount Laurel, New Jersey. Dr. Sullivan's present affiliation is Gribbles Veterinary Pathology, Glenside, South Australia. Dr. Sánchez's present affiliation is Antech Diagnostics, Lake Success, New York. This research did not receive any grant from funding agencies in the public, commercial or not-for-profit sectors.

Conflict of Interest Statement

The authors declare no conflicts of interest with respect to the publication of this manuscript.

Supplementary data

Supplementary data related to this article can be found at <http://dx.doi.org/10.1016/j.jcpa.2016.11.270>.

References

- Arnesen M, Manivel JC (1993) Plasmacytoma of the thoracic spine with intracellular amyloid and massive extracellular amyloid deposition. *Ultrastructural Pathology*, **17**, 447–453.
- Chaffin K, Cross AR, Allen SW, Mahaffey EA, Watson SK (1998) Extramedullary plasmacytoma in the trachea of a dog. *Journal of the American Veterinary Medical Association*, **212**, 1579–1581.
- dos Anjos Corvo MA, Granato L, Ikeda F, de Próspero JD (2013) Extramedullary nasal plasmacytoma: literature review and a rare case report. *International Archives of Otorhinolaryngology*, **17**, 213–217.
- Greenberg MJ, Schatzberg SJ, deLahunta A, Stokol T, Summers BA (2004) Intracerebral plasma cell tumor in a cat: a case report and literature review. *Journal of Veterinary Internal Medicine*, **18**, 581–585.
- Gross TL, Ihrke PJ, Walder EJ, Affolter VK (2005) Lymphocytic tumors. In: *Skin Diseases of the Dog and Cat*, 2nd Edit., TL Gross, PJ Ihrke, EJ Walder, VK Affolter, Eds., Blackwell Publishing Company, Odder, p. 871.
- Hayes AM, Gregory SP, Murphy S, McConnell JF, Patterson-Kane JC (2007) Solitary extramedullary plasmacytoma of the canine larynx. *Journal of Small Animal Practice*, **48**, 288–291.
- Johnson KH, Sletten K, Hayden DW, O'Brien TD, Rossow KD *et al.* (1995) AA amyloidosis in Chinese shar-pei dogs: immunohistochemical and amino acid sequence analyses. *Amyloid*, **2**, 92–99.
- Kyriazidou A, Brown PJ, Lucke VM (1989) Immunohistochemical staining of neoplastic and inflammatory plasma cell lesions in feline tissues. *Journal of Comparative Pathology*, **100**, 337–341.
- Majzoub M, Breuer W, Platz SJ, Linke RP, Hermanns W (2003) Histopathologic and immunophenotypic characterization of extramedullary plasmacytomas in nine cats. *Veterinary Pathology*, **40**, 249–253.
- Michau TM, Proulx DR, Rushton SD, Olivry T, Dunston SM *et al.* (2003) Intraocular extramedullary plasmacytoma in a cat. *Veterinary Ophthalmology*, **6**, 177–181.
- Platz SJ, Breuer W, Pflieger S, Minkus G, Hermanns W (1999) Prognostic value of histopathological grading in canine extramedullary plasmacytomas. *Veterinary Pathology*, **36**, 23–27.
- Ramos-Vara JA, Takahashi M, Ishihara T, Miller MA, Pace LW *et al.* (1998) Intestinal extramedullary plasmacytoma associated with amyloid deposition in three dogs: an ultrastructural and immunoelectron microscopic study. *Ultrastructural Pathology*, **22**, 393–400.
- Rowland PH, Linke RP (1994) Immunohistochemical characterization of lambda light-chain-derived amyloid in one feline and five canine plasma cell tumors. *Veterinary Pathology*, **31**, 390–393.
- Schöniger S, Bridger N, Allenspach K, Mantis P, Rest J *et al.* (2007) Sinonasal plasmacytoma in a cat. *Journal of Veterinary Diagnostic Investigation*, **19**, 573–577.
- Sharma N, Sharma S, Bindra R (2009) Plasmacytoma with amyloidosis masquerading as tuberculosis on cytology. *Journal of Cytology/Indian Academy of Cytologists*, **26**, 161–163.
- Snyder PW (2012) Diseases of immunity: amyloidosis. In: *Pathologic Basis of Veterinary Disease*, 5th Edit., JF Zachery, MD McGavin, Eds., Elsevier Mosby, St. Louis, pp. 284–288.
- Weigt AK, McCracken MD (2001) Extramedullary plasmacytoma in the canine trachea: case report and literature review. *Compendium on Continuing Education for the Practicing Veterinarian*, **23**, 143–152.
- Witham AI, French AF, Hill KE (2012) Extramedullary laryngeal plasmacytoma in a dog. *New Zealand Veterinary Journal*, **60**, 61–64.
- Zikes CD, Spielman B, Shapiro W, Roth L, Ablin L (1998) Gastric extramedullary plasmacytoma in a cat. *Journal of Veterinary Internal Medicine*, **12**, 381–383.

[Received, August 31st, 2016
Accepted, November 19th, 2016]